Crossref
DOI: 10.31643/2028/6445.01
Mining & Mineral Processing

Acid and Thermal Activation of Clay Separated from Kaoline for Uranium Purification

[1]Maldybayev G., [2]Gerassyova N., [1*]Sharipov R., [1]Zhangabayeva A., [1]El-Sayed Negim, [1]Khambarqyzy A., [1] Kylyshkanov M., [3] Bekbayeva L., [1] Balgimbayeva U., [4]Moshera Samy

[1]Kazakh British Technical University, Almaty, Kazakhstan
[2]LLC Deep Core Analytics, Almaty, Kazakhstan
[3]Al-Farabi Kazakh National University, Almaty, Kazakhstan
[4] National Research Centre, Dokki, Giza, Egypt

** Corresponding author email: r.sharipov@kbtu.kz*

Received: *February 28, 2026*
Peer-reviewed: *March 18, 2026*
Accepted: *April 2, 2026*

ABSTRACT
Clay minerals are commonly used as adsorbents due to their wide availability, large specific surface area, and cation exchange capabilities, making them suitable for removing heavy metal ions from wastewater. This study investigated the activation of clay by acid and thermal treatment to obtain an adsorbent for the purification of uranium from impurities such as iron and magnesium. Acid modification of clay samples was carried out with sulfuric acid (15%) at a temperature of 80–90 °C for 3 hours. While the activation of the clay using the thermal process was performed at 600–650 °C for 12–24 hours. X-Ray Diffraction, Electron Paramagnetic Resonance (EPR), and Fourier Transform Infrared Spectroscopy (FTIR) were used to analyse the clay's chemical composition and structural changes before and after activation. FTIR identified free OH groups and hydrated SiO2. EPR showed a high level of paramagnetic centers linked to structural defects and oxygen vacancies, which contribute to the material's strong adsorption and catalytic activity. After acid treatment, the clay particles exhibited a notable rise in specific surface area, expanding from 35.2 m^2/g to 342.5 m^2/g. Additionally, the specific pore volume grew substantially, increasing from 0.024 cm^3/g to 0.30 cm^3/g.

Keywords: clay, acid activation, thermal activation, uranium.

Information about authors:

Galymzhan Maldybayev — *PhD, Associate Professor, Laboratory of Advanced Materials and Technologies, Kazakh British Technical University, 050000, St. Tole bi, 59, Almaty, Kazakhstan. Email: g.maldybaev@kbtu.kz*

Gerassyova Natalya — *Doctoral student, LLC Deep Core Analytics, al-Farabi av., 17/1 b5B, 050059, Almaty, Kazakhstan. Email: tatoline2001@gmail.com*

Rustam Sharipov — *PhD, Assistant Professor, Laboratory of Advanced Materials and Technologies, Kazakh British Technical University, 050000, St. Tole bi, 59, Almaty, Kazakhstan. Email: r.sharipov@kbtu.kz*

Assem Zhangabayeva — *Researcher, Laboratory of Advanced Materials and Technologies, Kazakh British Technical University, 050000, St. Tole bi, 59, Almaty, Kazakhstan. Email: a.zhangabayeva@kbtu.kz*

El-Sayed Negim — *PhD, Professor, School of Materials Science and Green Technologies, Kazakh British Technical University, 050000, St. Tole bi, 59, Almaty, Kazakhstan. Email: elashmawi5@yahoo.com*

Aigerim Khambarqyzy — *Researcher, Laboratory of Advanced Materials and Technologies, Kazakh British Technical University, 050000, St. Tole bi, 59, Almaty, Kazakhstan. Email: a.khambarkyzy@kbtu.kz*

Manarbek Kylyshkanov — *Doctor of Physico-Mathematical Sciences, Laboratory of Advanced Materials and Technologies, Kazakh British Technical University, 050000, St. Tole bi, 59, Almaty, Kazakhstan. Email: kylyshkanov@mail.ru*

Lyazzat Bekbayeva — *PhD, Associate Professor, National Nanotechnology Open Laboratory, Al-Farabi Kazakh National University, 050040, Al-Farabi av., Almaty, Kazakhstan. Email: lyazzat_bk2019@mail.ru*

Ulpan Balgimbayeva — *PhD, Laboratory of Advanced Materials and Technologies, Kazakh British Technical University, 050000, St. Tole bi, 59, Almaty, Kazakhstan. Email: u.balgimbaeva@kbtu.kz*

Moshera Samy — *PhD, Polymers and Pigments Department, National Research Centre, 33 El Buhouth St., Dokki, Giza 12622, Egypt. Email: moshera_samy1984@yahoo.com; ORCID ID: https://orcid.org/0000-0002-7272-4134*

Introduction

In industrial water systems, silicon is present in multiple physicochemical forms based on different factors, including its solubility and degree of aggregation: as monomeric soluble silicon dioxide (SiO_2), as colloidal aggregates ($SiO_2 \cdot nH_2O$), and in the solid phase as sand, silt, or silicate minerals [[1], [2], [3]]. In uranium hydrometallurgy, the ionic and colloidal forms are dominant, significantly affecting the efficiency of technological processes, including sorption, equipment corrosion, and scale formation [4]. There are

different types of silicon depends on factors such as pH, temperature, ionic strength, and what's in the solution. When uranium ores undergo in-situ leaching with sulfuric acid, silicon primarily dissolves as an impurity that reduces the efficiency of uranium extraction [4]. Sulfuric acid ion exchange process for uranium ores reacts with aluminosilicate minerals such as kaolinite, chlorite, hydromica, and coffinite, producing silicic acid that can polymerize into high-molecular-weight compounds [6]. These compounds accumulate and infiltrate in anion exchange resins, causing significant improvement in silicification, reducing uranium capacity, increasing hydraulic resistance, impeding desorption and denitration, and degrading mechanical properties. Silicon content in waste resins may reach 12–15 wt.%, so removal is necessary either before sorption or from saturated resins [[7], [8]]. Several methods are available for removing silicon from industrial solutions, including adsorption, ion exchange, reverse osmosis, electrodialysis, chemical precipitation, and extraction [[3], [4],[4]]. In uranium environments, adsorption is preferred due to its selectivity and cost-effectiveness. It offers low energy use, adsorbent regeneration, environmental safety, and process flexibility. Adsorption may occur through physical forces (van der Waals) or chemisorption, which forms stronger chemical bonds between the adsorbate and adsorbent [[2], [9], [10]]. Physical adsorption occurs due to weak intermolecular forces and the condensation of molecules within the pores of a solid, whereas chemical adsorption (chemisorption) involves the formation of chemical bonds between the sorbate molecule and the active sites on the adsorbent surface on the adsorbent surface [[2],[11]]. Chemisorption results in the formation of an adsorbate monolayer and is often irreversible, making it particularly effective for the deep extraction of target components. A thorough understanding of adsorption mechanisms is necessary for both the design and optimization of industrial processes, as well as for the accurate characterization of the porous structure of materials [12]. Ion exchange is used to purify, separate, and recover ion-containing solutions using solid materials such as resins, membranes, and minerals. However, this method requires significant capital and operating costs, especially when resin regeneration and waste disposal are required [[13], [14], [15], [16]]. Chemical precipitation is used to convert dissolved substances into a solid phase, but is ineffective for removing trace contaminants and produces large amounts of sludge requiring further processing [[14], [15]]. Reverse osmosis is a membrane process that uses pressure to selectively remove ions and molecules through a semipermeable membrane. Electrodialysis allows for the selective extraction of ions using an electric field, but also produces concentrated waste streams [[15], [16], [17], [18]. It is effective for desalination but is limited in application due to the high cost of the membranes and sensitivity to fouling [[19], [20], [21]]. Electrolysis is used to extract elements from solutions but has limited application in the context of silicon removal [22], [23], [24], [25]]. Sulfuric acid in-situ leaching of uranium ores results in the transfer of uranium and several other elements from the ore-bearing rocks into the productive solution, leading to contamination of the productive solutions with ballast impurities. During the sorption extraction of uranium, these impurities behave differently and can be classified according to their behavior as inert, depressant, or toxic. In sulfuric acid environments, silicic acid is the most significant toxic impurity. The transfer of silicon into productive solutions is caused by reactions between sulfuric acid and aluminosilicates, chlorites, hydromicas, and the uranium-bearing mineral coffinite.

The goal of this study is to develop process modes and parameters for producing effective chemical adsorbents based on an aluminosilicate carrier, as well as to study the distribution and behavior of silicon in uranium sorption processing cycles.

Experimental part

Materials

Samples of kaolin ore from the Kostanay region were preliminarily crushed using a jaw crusher, Allis Mineral Systems (model N184T17FB12C), until a particle size was achieved at which all the material passed through a sieve with an aperture of 0.074 mm. The resulting crushed material was then processed in a Denver flotation cell equipped with a two-blade impeller. During processing, water was added to obtain a dense, homogeneous pulp; the solids content was not quantitatively controlled. At the final stage, the pulp was subjected to sieve analysis using Tyler sieves with additional dilution by water.

Method for separating clay and sand fractions from kaolin ore

The reactivity and practical of minerals are largely determined by the degree of structural order within their crystal lattices. The diversity of layered silicates stems from the presence of not only silicon–oxygen tetrahedra but also aluminum - and iron – oxygen tetrahedra. When tetravalent silicon (Si^{4+}) is substituted by trivalent aluminum (Al^{3+}), charge neutrality must be preserved through the

incorporation of compensating cations such as K^+, Na^+, or Ca^{2+}. The formation of active centers requires the gradual disruption of polyaluminosilicate frameworks. As a result, the process flow has been improved by introducing a preliminary separation of the ore into clay and sand fractions using a hydrocyclone system [[26], [27], [28], [29], [30]]. The results of test trials on clay–sand separation are presented in Table 1.

Table 1 shows that ore separation concentrates about 30% Al_2O_3 and 50% SiO_2 of the feedstock mass in the clay fraction. The conversion of Al_2O_3 into the clay fraction reaches 60–80%. As a result, adding the siphon separation step to ore preparation significantly impacts the process on a large scale; it mechanically activates the material, essentially "shaking" the aluminosilicate structures. Acid activation of the original clay mass.

Acid activation removes Fe and Mg impurities, breaks down inert minerals, and increases the surface area and porosity of clay, enhancing its adsorption and catalytic properties.

When treated with sulfuric acid (H_2SO_4), oxides and hydroxides of transition and alkaline earth metals are converted into soluble sulfate forms:

$$Fe_2O_3 + 3\ H_2SO_4 \rightarrow Fe_2(SO_4)_3 + 3\ H_2O$$
$$MgO + H_2SO_4 \rightarrow MgSO_4 + H_2O$$

Furthermore, controlled acid treatment facilitates the partial removal of adsorbed impurities and improves access to the material's pore system. However, excessively intense treatment can leach out structural aluminum and destroy the underlying aluminosilicate lattice, resulting in reduced product quality. Therefore, it is necessary to carefully control the acid concentration, process temperature, treatment duration, and solid-to-liquid ratio.

Preliminary modification of the structure and properties of mineral raw materials under the influence of chemical and physical factors creates optimal conditions for subsequent leaching and the formation of a developed porous structure.

To perform the acid treatment, 100 g of calcined and crushed clay material was loaded into the reactor, then 1 liter of a 15% H_2SO_4 solution was added at room temperature, and the system was heated to 80-90 °C. The process was carried out with vigorous stirring (~300 rpm) for 3 hours, with periodic sampling of the solid and liquid phases at 30, 60, 120, and 180 minutes to assess the reaction kinetics. Upon completion of the treatment, the mixture was cooled to ~40 °C and filtered, separating the liquid and solid phases.

The precipitate was washed with several portions of water until the filtrate pH reached approximately 6.5–7.0 and the conductivity was close to the initial value, monitoring the parameters with a pH meter. The purified solid residue was dried at 105 °C to constant weight.

Table 1 – Technological parameters of siphon-based ore separation: sieve analysis of the feed ore, detailing the mass fractions of aluminum and silicon within the size classes of both the hydrocyclone overflow and underflow (sand) streams.

No.	Separation product	Tormentation		Al_2O_3		Distribution Al_2O_3	SiO_2		Distribution SiO_2
		G	%	%	G	%	%	G	%
1	Raw ore	1866	100	20.97	391.3		60.75	1133	
	Clay	1323	71	23.95	316.8	81	56.78	751	66.3
	Sands	543	29	13.72	74.5	19	70.35	382	33.7
2	Raw ore	1855	100	22.24	412.5		61.4	1138	
	Clay	1292	69.6	25.91	334.75	81.1	56.72	732	64.3
	Sands	563	30.4	13.81	77.75	18.9	72.11	406	35.7
3	Source ore	3256	100	20.72	674.6		60.38	1965	
	Clay	1463	45	30.32	443.5	65.8	46.42	679	34.55
	Sands	1793	55	12.88	231.1	34.2	71.7	1286	65.44
4s	Raw ore	1960	100	22.88	448.4		56.12	1099	
	Clay	848.8	43.3	30.1	255.5	57	47.52	403	36.7
	Sands	1111.2	56.7	17.35	192.9	43	62.63	696	63.3

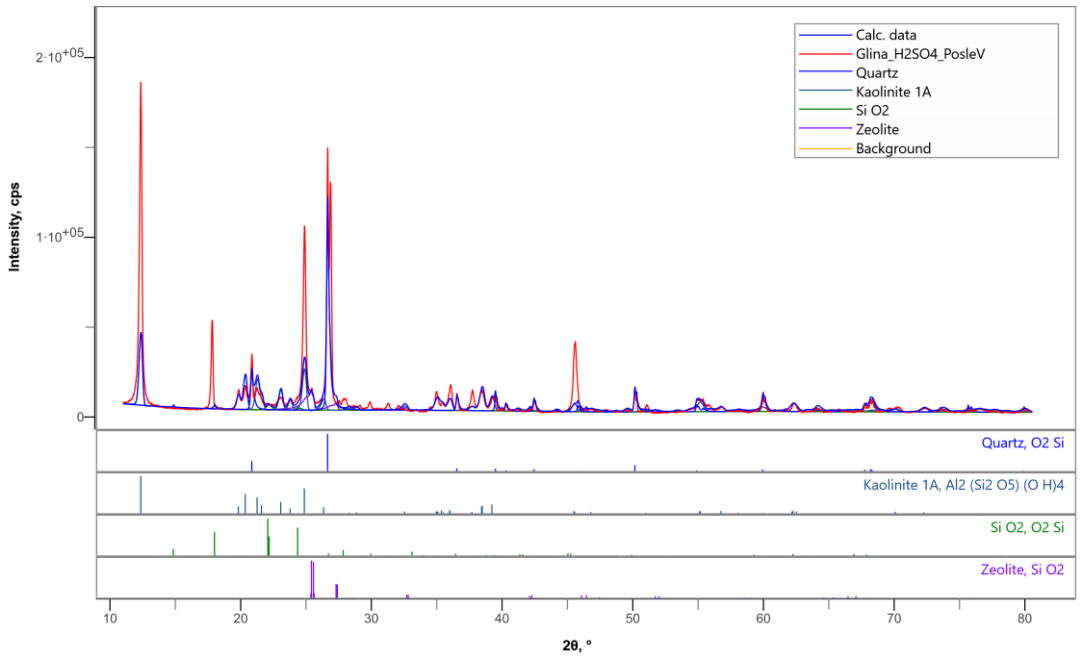

Figure 1 – X-ray diffraction pattern of kaolin clay after leaching

Table 2 – Phase composition of the sample determined by XRD

Component		Formula	Mass fraction, %
A	Quartz	SiO_2	33.7
B	Kaolinite 1A	$Al_2(Si_2O_5)(OH)_4$	50.7
C	Silicon dioxide	SiO_2	2.4
D	Zeolite	SiO_2	13.2

Figure 1 and Table 2 X-ray diffraction (XRD) analysis results show that the resulting material does not meet the expected characteristics required to form an active component based on the metakaolin mineral. This result indicates incomplete transformation of the original kaolinite into metakaolin, which may be due to insufficient dehydroxylation. Furthermore, the potential for the formation of secondary silicate compounds leads to a decrease in the proportion of free aluminum oxide in the composition. These deviations limit the potential for further use of the material as a chemical adsorbent.

Thermal activation of kaolin clay

Thermal activation of clay minerals involves treating natural clay at elevated temperatures, which causes the removal of adsorbed gases and water molecules and leads to the formation of a free surface. However, upon reaching certain temperatures characteristic of each specific mineral, the crystal lattice can partially disintegrate or completely collapse, which reduces the surface activity of the material. Based on the results of differential thermal analysis and thermogravimetry, it was established that the sample contains: quartz - less than 40%, kaolinite - about 50%, hydromica - 4.4%, chlorite - less than 1%, goethite - 1.6%, as well as thermally inert components - less than 5%. When heated, the characteristic features of the thermal behavior of these minerals did not show noticeable differences from the behavior of the components of the original ore.

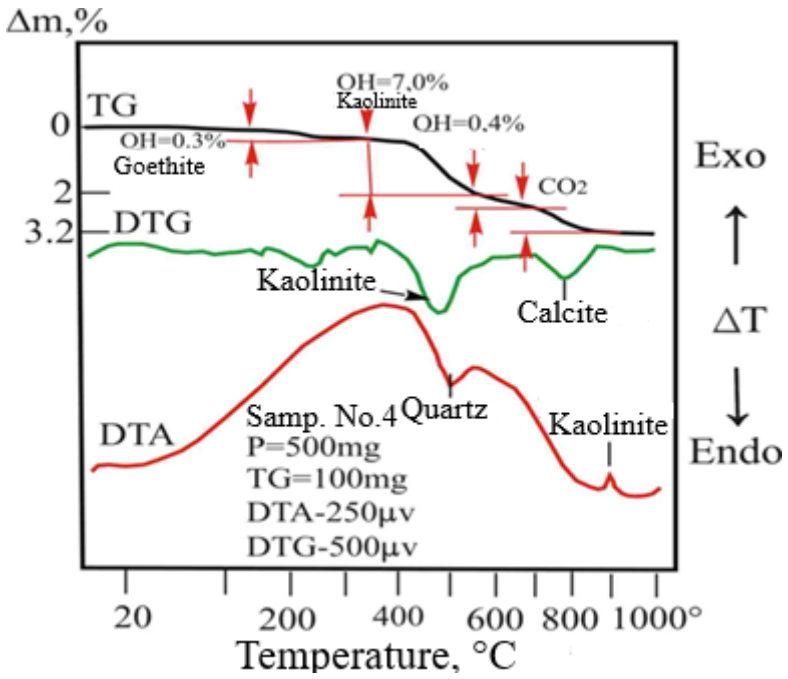

Mineral composition: quartz <80%, kaolinite – 12.1%, mica – 2.5%, goethite – 1.6%, calcite – 1.8%, TIM ~5%

Figure 2 - Derivative diagram of the clay fraction

Table 3 - Mineral and material composition of kaolin ore based on the results of thermal analysis

Sample name	Mineral and material composition of rocks, %													PP, 1000º C, %
	Quartz	Kaolinite	Hydromica	Mica	Chlorite	Calcite	Goethite	Hematite	TIM	Other minerals	H_2O	HE	CO_2	
Aluminosilicate carrier	<40	50.0	4.4	0.3	<1	-	1.6	-	5.0	-	0.4	7.8	-	8.2
Note: TIM – thermally inert minerals PS, diopside, etc. PPP –loss on ignition														

Figure 2 and Table 3 illustrate the results of DTA-TG-DTG analysis, which confirm the presence of hydroxyl and carbonate compounds in the sample and also allow us to determine the optimal range of thermal activation temperatures – from 600 to 700 °C, at which the dehydroxylation of kaolinite is completed and reactive metakaolin is formed without significant loss of structure and with the preservation of active adsorption centers. Up to 200 °C, a slight decrease in mass is observed, associated with the removal of physically adsorbed moisture and dehydration of the mineral surface. Around 250 °C - a small change in mass due to the removal of hydroxyl groups from goethite (OH ≈ 0.3%). In the range of 400–550 °C, there is an intense endothermic decrease in mass associated with the dehydroxylation of kaolinite (OH ≈ 7%), which leads to the formation of metakaolin. Around 600 °C, there is a weak peak of mica dehydroxylation (OH ≈ 0.4%). In the range of 700–850 °C, CO_2 is released,

corresponding to the decomposition of calcite ($CaCO_3 \rightarrow CaO + CO_2$). Above 900 °C, recrystallization of kaolinite begins with the formation of high-temperature phases (mullite, quartz) [[31], [32]].

Thus, thermal activation of clay minerals is possible at temperatures above 500°C. Puncture losses contribute to the formation of voids and new active centers, the structural elements of which in zeolites are SiO_4 and AlO_4 tetrahedra, connected at their corners to form cavities and channels through which hydrated cations, water, and other molecules can diffuse [33].

Based on the above, the solid product after leaching was subjected to additional thermal activation at 600–650 °C for 12–24 hours to stabilize the structure and increase the specific surface area. The resulting activated material was analyzed using X-ray diffraction (XRD), as shown in Figure 3 and Table 4.

X-ray diffraction analysis revealed that after heat treatment, partial amorphization of the aluminosilicate component was observed in the sample, accompanied by the disappearance of characteristic kaolinite reflections. This confirms the formation of metakaolin—an amorphous, reactive phase formed through dehydroxylation and the breakdown of the mineral's layered structure. The diffraction pattern reveals an increase in the amorphous background in the 15–35° 2θ range, reflecting an increase in the number of defective structural regions acting as active adsorption sites. The remaining quartz reflections and minor iron silicate peaks correspond to thermally stable impurities that do not participate in the formation of the active component. Thus, the resulting metakaolin possesses a developed defective surface capable of effectively binding silicon in solutions and providing increased sorption activity.

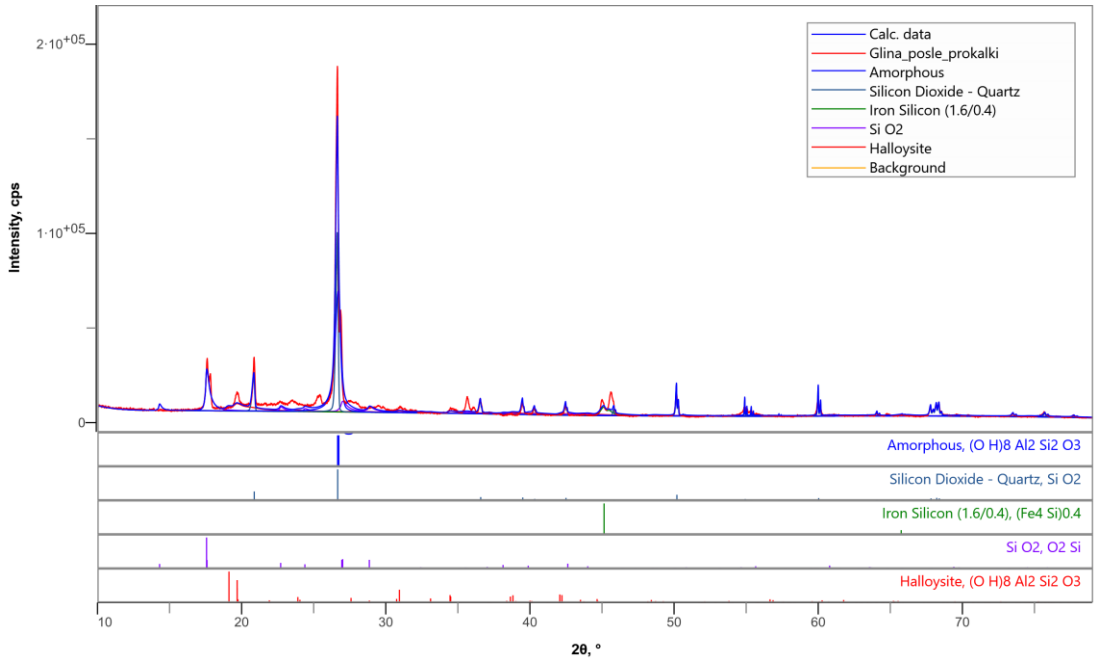

Figure 3 – X-ray diffraction pattern of kaolin clay after heat treatment

Table 4 – Phase composition of the sample determined by XRD

Component		Formula	Mass fraction, %
A	Silicon dioxide - Quartz	SiO_2	34.96
B	Iron silicide (1.6/0.4)	$(Fe_4Si)_{0.4}$	2.74
C	Silicon dioxide	SiO_2	26.2
D	Metakaolin	$Al_2Si_2O_3(OH)_8$	36.1

Results and Discussion

FT-IR analysis of the obtained chemical adsorbent

The predominance of hydrated silica indicates a highly amorphous matrix with inclusions of crystalline Al and Fe phases (metakaolin). This combination of phases explains the observed combination of broad background bands and several sharp peaks in XRD/IR: amorphous SiO_2 provides the background "flat" component, while the crystalline phases are responsible for the narrow peaks and characteristic OH/Si–O peaks. For technological applications, this implies high reactivity and absorption capacity (due to hydrated SiO_2), as well as the presence of stable mineral phases that influence thermal stability and behavior during heat treatment/chemical extraction.

The absorption spectrum in Figure 4 exhibits various vibrations above 3000 cm^{-1}. Absorption at 3400 cm^{-1} is attributed to absorbed water in the bulk phase (film water and water in inclusions), while the region around 3304 cm^{-1} is associated with the absorption of water molecules disturbed by the crystal's surface field. Under the influence of this field, the distances between the charges of water's molecular dipoles are slightly increased compared to the average distance in the bulk phase. This reduces bond rigidity and the vibration frequency.

Absorption at 3478 cm^{-1} in kaolin clay is characteristic of molecular water. Deformation vibrations of H_2O in mineral crystals are observed at higher frequencies (1620 cm^{-1}). This is attributed to the fact that water molecules in the crystal are bound by stronger hydrogen bonds.

The absorption band for the practically free OH group in kaolinite is around ~3600 cm^{-1}, the absorption band of water is around ~3450 cm^{-1}, and the absorption band for short hydrogen bonds O-H...O is around ~3300 cm^{-1}. The spectrum band of 1620 cm^{-1} is related to the deformation vibrations of the OH bond. Thus, the crystalline form of the original product is transformed predominantly into an ionic state, which determines the physicochemical properties of the leaching residue.

Study of the specific surface area and porosity of the chemical adsorbent

The specific surface area and pore structure parameters of the original kaolin clays and the resulting chemical adsorbent were studied using low-temperature nitrogen adsorption using the BET method. The results show a significant change in textural characteristics after activation treatment (Table 5). The measurements were performed using a SORBTOMETR-M instrument.

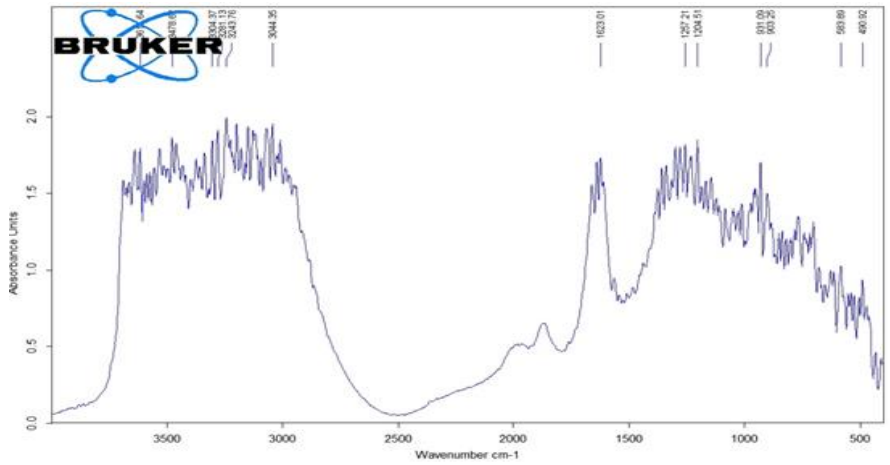

Figure 4 – FTIR spectra of chemical adsorbent

Table 5 – Specific surface area, specific volume and average pore size of the active component

Sample	Specific surface area, m^2/g	Specific pore volume, cm^3	Average pore size, angstroms
Original kaolin	35.2	0.024	1.52
Chemical adsorbent	342.5	0.30	1.95

The starting material has a relatively low specific surface area of 35.2 m²/g, a small specific pore volume (0.024 cm³/g), and an average pore size of about 1.52 Å, which corresponds to the dense, poorly developed porous structure of the natural mineral.

After activation, a sharp increase in the specific surface area to 342.5 m²/g is observed, exceeding the initial value by more than an order of magnitude. The specific pore volume increases to 0.30 cm³/g, indicating significant development of the microporous and mesoporous structure. The average pore size remains virtually unchanged (1.95 Å), indicating that the treatment primarily increases the number of active pores rather than changes their size.

Thus, the activation treatment ensures the formation of a highly developed porous structure, significantly increasing the specific surface area of the material. This directly enhances the effectiveness of the active component as a sorbent, improving the accessibility of active sites and the adsorption capacity of the material.

Study of the patterns of occurrence, content, and form of silicon compounds at different stages of processing uranium-containing solutions

To study methods for neutralizing silicon poisoning of the resin, the behavior of silicon in a uranium-containing solution was first studied. Silicon dioxide, SiO_2, is the anhydride of a series of silicic acids, whose composition can be expressed by the general formula $xSiO_2 \times yH_2O$, where x and y are integers.

x = 1, y = 1:$SiO_2 \times H_2O$, i.e. H_2SiO_3 – metasilicic acid;

x = 1, y = 2:$SiO_2 \times 2H_2O$, i.e. H_4SiO_4 – orthosilicic acid;

x = 2, y = 1:$2SiO_2 \times H_2O$, i.e. $H_2Si_2O_5$ – dimethylsilicic acid.

According to many researchers, the solubility of silicic acid at room temperature is 0.01–0.017% (calculated as SiO_2). As the temperature increases, its solubility increases, reaching 0.04% at 94 °C. Silicic acid is a very weak electrolyte. Its dissociation constant is 2×10-10. The pH of an aqueous silicic acid solution is approximately 4.0–4.5. Data on the solubility of amorphous silicon dioxide are presented in Table 6.

In natural waters, silicon compounds are found in dissolved, suspended, and colloidal states, the quantitative relationships between which are determined by the chemical composition of the water, temperature, pH, and other factors.

The dissolved forms are mainly represented by molecular orthosilicic acid $H_4SiO_4(SiO_2 \cdot 2H_2O)$, metasilicic $H_2SiO_3(SiO_2 \cdot H_2O)$, disilicic $H_2Si_2O_5$ $(2SiO_2 \cdot H_2O)$, and other acids with different numbers of SiO_2 and H_2O, products of their dissociation and association, as well as silicon-organic compounds. Polymeric and colloidal forms of silicic acid have a variable composition of the type $mSiO_2\ nH_2O$ (m and n are integers).

In aqueous solutions, the monomer silicic acid can be found primarily in five forms: H_4SiO_4, H_3SiO^{4-}, $H_2SiO_4^{2-}$, $HSiO_4^{3-}$, and SiO_4^{4-}. The ratio of silicic acid forms in water is determined by the dissociation constants of each of the stages. Figure 5 shows the dependence of the distribution of forms of dissolved silicon on the pH of the environment, from which it follows that in natural waters, the main part of silicic acid is in a molecularly dissolved form.

Therefore, during ion exchange, silicon begins to be absorbed as the medium transitions to an alkaline region, where it exists in an ionic form. This is achieved in practice by a highly basic anion exchange resin in the absence of strong acid anions. Thus, silicon in a process uranium-containing solution in the pH range up to 8.0 is monosilicic acid, which undergoes a polycondensation reaction as shown in Figure 5. In the pH range of 2.0 to 3.0, the polycondensation rate is minimal. Silicic acid cannot react chemically with other elements up to a pH of 8.0.

Table 6 – Dependence of the solubility of amorphous silicon dioxide on the pH of the solution at 25 °C

pH	1.0	2.0	3.0	4.2	5.7	7.7	10.26	10.6
Solubility, %	0.014	0.015	0.015	0.013	0.011	0.010	0.019	0.112

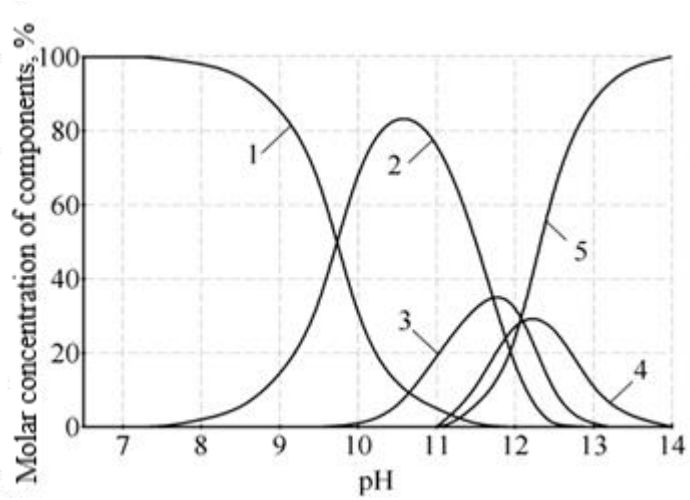

1 – H_4SiO_4; 2 – $H_3SiO_4^-$; 3 – $H_2SiO_4^{2-}$; 4 – $HSiO_4^{3-}$; 5 – SiO_4^{4-}

Figure 5 – Dependence of the ratio of silicic acid forms on the pH of the medium

Conclusions

The process modes for producing the active component for synthesizing chemical adsorbents based on kaolin or were developed. Hydrocyclone separation of kaolin ore enabled enrichment of the clay fraction in Al_2O_3 to 60–80% of the total content in the feedstock, ensuring high reactivity of subsequent products. Acid activation of the resulting clay mass with sulfuric acid (15%, 80–90 °C, 3 h) allowed for the partial removal of iron and magnesium impurities, increasing the availability of the aluminosilicate structure for further modification. To form the active phase, metakaolin-heat treatment was performed at 600–650 °C for 12–24 hours. The results of differential thermal analysis (DTA-TG-DTG) and X-ray diffraction (XRD) confirmed the completion of kaolinite dehydroxylation and the formation of an amorphous, reactive phase with a defective structure capable of effectively interacting with silicon compounds. The phase composition of the final product includes quartz (34.96%), metakaolin (36.1%), and amorphous silicon dioxide (26.2%), which meets the requirements for materials used as sorbents. The physicochemical characteristics of the obtained chemical adsorbent showed a significant improvement in textural properties compared to the original kaolin: the specific surface area increased from 35.2 m^2/g to 342.5 m^2/g, and the specific pore volume increased from 0.024 cm^3/g to 0.30 cm3/g. This indicates the formation of a developed microporous structure, ensuring high accessibility of active centers for sorption. IR spectroscopy confirmed the presence of free OH groups and hydrated forms of SiO_2.

Conflicts of interest. Authors declare no conflict of interest.

CRediT author statement: G. Maldybayev, N. Gerassyova: Conceptualization, Methodology, Software. R. Sharipov: Data curation, Writing draft preparation.: Visualization, Investigation. A. Zhangabayeva: Supervision. E. Negim: Software, Validation. A. Khambarqyzy, M. Kylyshkanov, L. Bekbayeva, U. Balgimbayeva U, M. Samy: Reviewing and Editing.

Acknowledgements. This research was funded by the Committee of Science of the Ministry of Science and Higher Education of the Republic of Kazakhstan (Grant No. BR28713471 Development of methods for increasing the extraction of uranium from uranium-containing solutions by effectively reducing the content of silicon compounds).

Cite this article as: Maldybayev G, Gerassyova N, Sharipov R, Zhangabayeva A, El-Sayed Negim, Khambarqyzy A, M. Kylyshkanov, Bekbayeva L, Balgimbayeva U, Moshera Samy. Acid and Thermal Activation of Clay Separated from Kaoline for Uranium Purification. Kompleksnoe Ispolzovanie Mineralnogo Syra = Complex Use of Mineral Resources. 2028; 344(1):5-17. https://doi.org/10.31643/2028/6445.01

Уранды тазарту үшін каолиннен бөлінген саздың қышқылды және термиялық активтенуі

[1] Малдыбаев Ғ., [2]Герасёва Н., [1] Шарипов Р., [1] Жаңабаева Ә., [1]El-Sayed Negim, [1]Хамбарқызы Ә., [1] Қылышқанов М., [3] Бекбаева Л., [1] Балгимбаева У., [4]Moshera Samy

[1] Қазақстан- Британ Техникалық Университеті Алматы, Қазақстан
[2]ЖШС Deep Core Analytics, Алматы, Қазақстан
[3] Әл-Фараби атындағы Қазақ Ұлттық Университеті, Алматы, Қазақстан
[4] Ұлттық зерттеу орталығы, Докки, Гиза, Египет

Мақала келді: *28 ақпан 2026*
Сараптамадан өтті: *18 наурыз 2026*
Қабылданды: 2 *сәуір 2026*

Саз минералдарын әдетте адсорбенттер ретінде пайдаланылады, себебі олар қолжетімді және аумақты меншікті бет ауданында катион алмасу қабілетіне байланысты адсорбент ретінде кеңінен қолданылады, бұл оларды ағынды сулардан ауыр металл иондарын кетіруге жарамды етеді. Бұл зерттеу темір мен магний сияқты қоспалардан уранды тазартуға арналған қоспа алу үшін саздың қышқыл мен және термиялық өңдеу арқылы активтенуін зерттеді. Саз үлгілерінің қышқылдық модификациясы күкірт қышқылымен (15%) 80-90 °C температурада 3 сағат бойы жүргізілді. Сазды термиялық процестің көмегімен активтендіру 600-650 °c температурада 12-24 сағат ішінде жүргізілді. Саздың химиялық құрамын және активацияға дейін және одан кейінгі құрылымдық өзгерістерді талдау үшін рентгендік дифракция, электронды парамагниттік резонанс (ЭПР) және Фурье түрлендіруінің инфрақызыл спектроскопиясы (FTIR) қолданылды.Бос ОН топтары және гидратталған SiO_2 FTIR көмегімен анықталды. ЭПР құрылымдық ақауларымен және оттегінің жетіспеушілігімен байланысты парамагниттік орталықтардың жоғары деңгейін көрсетті, бұл материалдың күшті адсорбциясы мен каталитикалық белсенділігіне ықпал етеді. Қышқылмен өңдеуден кейін саз бөлшектерінің меншікті беткі ауданы 35,2 $м^2$/г-нан 342,5 $м^2$/г-ға дейін кеңейіп айтарлықтай өсуін көрсетті. Сонымен қатар, кеуектердің меншікті көлемі айтарлықтай өсіп, 0,024 $см^3$/г-нан 0,30 $см^3$/г-ға дейін өсті.

Түйінді сөздер: саз, қышқылды активтендіру, термиялық активтендіру, уран.

Авторлар туралы ақпарат:

Ғалымжан Малдыбаев *PhD, қауымдастырылған-профессор, Перспективті Материалдар мен Технологиялар зертханасы, Қазақстан-Британ Техникалық Университеті, 050000, Төле би көшесі, 59, Алматы, Қазақстан. Email: g.maldybaev@kbtu.kz*

Наталья Герасёва *Докторант, ЖШС Deep Core Analytics, 050059, Аль-Фараби даңғылы, 17/1 к5Б, Алматы, Қазақстан. Email: tatoline2001@gmail.com*

Рустам Шарипов *PhD, ассистент-профессор, Перспективті Материалдар мен Технологиялар зертханасы, Қазақстан-Британ Техникалық Университеті, 050000,Төле би көшесі, 59, Алматы, Қазақстан. Email: r.sharipov@kbtu.kz*

Әсем Жаңабаева *Ғылыми қызметкер, Перспективті Материалдар мен Технологиялар зертханасы, Қазақстан-Британ Техникалық Университеті, 050000,Төле би көшесі, 59, Алматы, Қазақстан. Email: a.zhangabayeva@kbtu.kz*

El-Sayed Negim *PhD, Материалтану және жасыл технологиялар мектебінің профессоры, Қазақстан-Британ Техникалық Университеті, 050000, Төле би көшесі, 59, Алматы, Қазақстан. Email: elashmawi5@yahoo.com*

Әйгерім Хамбарқызы *Ғылыми қызметкер, Перспективті Материалдар мен Технологиялар зертханасы, Қазақстан-Британ Техникалық Университеті, 050000,Төле би көшесі, 59, Алматы, Қазақстан. Email: a.khambarkyzy@kbtu.kz*

Манарбек Кылышканов *Физ.-мат. ғ. докторы, Перспективті Материалдар мен Технологиялар зертханасы, Қазақстан-Британ Техникалық Университеті, 050000, Төле би көшесі, 59, Алматы, Қазақстан. Email: kylyshkanov@mail.ru*

Ләззат Бекбаева *PhD, қауымдастырылған-профессор, Ашық Түрдегі Нанотехнологиялық Зертхана, Әл-Фараби атындағы Қаз¥У, 050040, әл-Фараби даңғылы, 71, Алматы, Қазақстан. Email: lyazzat_bk2019@mail.ru*

Улпан Балгимбаева *PhD, Ғылым және инновациялар департаменті, Коммерцияландыру секторы, Қазақстан-Британ Техникалық Университеті, 050000, Төле би көшесі, 59, Алматы, Қазақстан. Email: u.balgimbaeva@kbtu.kz*

Moshera Samy *PhD, Полимерлер мен пигменттер кафедрасы, Ұлттық зерттеу орталығы, Әл-Бухут көшесі, 33, Докки, Гиза, 12622, Египет. Email: moshera_samy1984@yahoo.com; ORCID ID: https://orcid.org/0000-0002-7272-4134*

Кислотная и термическая активация глины, выделенной из каолина, для очистки урана

[1] Малдыбаев Г., [2]Герасёва Н., [1] Шарипов Р., [1] Жанабаева А., [1]El-Sayed Negim, [1]Хамбаркызы А., [1] Кылышканов М., [3] Бекбаева Л., [1] Балгимбаева У., [4]Moshera Samy

[1] Казахстанско-Британский технический университет, Алматы, Казахстан
[2]ТОО Deep Core Analytics, Алматы, Казахстан
[3]Казахский национальный университет им. Аль-Фараби, Алматы, Казахстан
[4]Национальный исследовательский центр, Докки, Гиза, 12622, Египет

Поступила: *28 февраля 2026*
Рецензирование: *18 марта 2026*
Принята в печать: *2 апреля 2026*

АННОТАЦИЯ

Глинистые минералы широко используются в качестве адсорбентов из-за их широкой доступности, большой удельной поверхности и способности к катионообмену, что делает их пригодными для удаления ионов тяжелых металлов из сточных вод. В этом исследовании изучалась активация глины кислотой и термической обработкой с получением добавки для очистки урана от примесей, таких как железо и магний. Кислотную модификацию образцов глины проводили серной кислотой (15%) при температуре 80-90°C в течение 3 часов. В то время как активацию глины термическим способом проводили при температуре 600-650°C в течение 12-24 часов. Для анализа химического состава глины и структурных изменений до и после активации были использованы методы рентгеновской дифракции, электронного парамагнитного резонанса (ЭПР), инфракрасной спектроскопии с преобразованием Фурье (ИК-ФУРЬЕ). С помощью ИК-ФУРЬЕ были определены свободные ОН-группы и гидратированный SiO_2. ЭПР показал высокий уровень парамагнитных центров, связанных со структурными дефектами и кислородными вакансиями, которые способствуют сильной адсорбционной и каталитической активности материала. После кислотной обработки удельная поверхность глинистых частиц заметно увеличилась с 35,2 $м^2$/г до 342,5 $м^2$/г. Кроме того, существенно увеличился удельный объем пор, увеличившись с 0,024 $см^3$/г до 0,30 $см^3$/г.

Ключевые слова: глина, кислотная активация, термическая активация, уран.

Информация об авторах:

Галымжан Малдыбаев — *PhD, Ассоциированный-профессор, Лаборатория перспективных материалов и технологий, Казахстанско-Британский технический университет, 050000, ул. Толе би, 59, Алматы, Казахстан. Email: g.maldybaev@kbtu.kz*

Наталья Герасёва — *Докторант, ТОО Deep Core Analytics, проспект Аль-Фараби, 17/1 к5Б, 050059, Алматы, Казахстан. Email: tatoline2001@gmail.com*

Рустам Шарипов — *PhD, Ассистент-профессор, Лаборатория перспективных материалов и технологий, Казахстанско-Британский технический университет, 050000, ул. Толе би, 59, Алматы, Казахстан. Email: r.sharipov@kbtu.kz*

Асем Жанабаева — *Научный сотрудник, Лаборатория перспективных материалов и технологий, Казахстанско-Британский технический университет, 050000, ул. Толе би, 59, Алматы, Казахстан. Email: a.zhangabayeva@kbtu.kz*

El-Sayed Negim — *PhD, Профессор Школы материаловедения и зеленых технологий, Казахстанско-Британский технический университет, 050000, ул. Толе би, 59, Алматы, Казахстан. Email: elashmawi5@yahoo.com*

Айгерим Хамбаркызы — *Научный сотрудник, Лаборатория перспективных материалов и технологий, Казахстанско-Британский технический университет, 050000, ул. Толе би, 59, Алматы, Казахстан. Email: a.khambarkyzy@kbtu.kz*

Манарбек Кылышканов — *Д.физ.-мат.наук, Лаборатория перспективных материалов и технологий, Казахстанско-Британский технический университет, 050000, ул. Толе би, 59, Алматы, Казахстан. Email: kylyshkanov@mail.ru*

Ляззат Бекбаева — *PhD, Ассоциированный-профессор, Лаборатория нанотехнологии открытого типа, КазНУ им. Аль-Фараби, 050040, проспект Аль-Фараби, 71, Алматы, Казахстан. Email: lyazzat_bk2019@mail.ru*

Улпан Балгимбаева — *PhD, Департамент науки и инноваций, Сектор коммерциализации, Казахстанско-Британский технический университет, 050000, ул. Толе би, 59, Алматы, Казахстан. Email: u.balgimbaeva@kbtu.kz*

Moshera Samy — *PhD, Кафедра полимеров и пигментов, Национальный исследовательский центр, ул. Эль-Бохут, 33, Докки, Гиза, 12622, Египет. Email: moshera_samy1984@yahoo.com; ORCID ID: https://orcid.org/0000-0002-7272-4134*

References

[1] Teng W, Liu S, Zhang X, Zhang F, Yang X, Xu M, Hou J. Reliability Treatment of Silicon in Oilfield Wastewater by Electrocoagulation. Water. 2023; 15:206. https://doi.org/10.3390/w15010206

[2] Kylyshkanov M, Gerassyova N, Sharipov R, Kuanysh A, Maldybayev G, Negim E-S, Baigenzhenov O, Bekbayeva L, Al Azzam K, & Balgimbayeva U. Innovative Adsorbent Materials for Efficient Silicon Extraction from Industrial Waters: A review. Kompleksnoe Ispolzovanie Mineralnogo Syra = Complex Use of Mineral Resources. 2025; 341(2):105–116. https://doi.org/10.31643/2027/6445.22

[3] Wang XJ, Goual L, Colberg PJS. Characterization and treatment of dissolved organic matter from oilfield produced waters. J. Hazard. Mater. 2012; 217:164–170.

[4] Fu F, Wang Q. Removal of heavy metal ions from wastewaters: A review. Journal of Environmental Management. 2011; 92(3):407-418. https://doi.org/10.1016/j.jenvman.2010.11.011

[5] Hubicki Z, Kolodynska D. Selective Removal of Heavy Metal Ions from Waters and Waste Waters Using Ion Exchange Methods. Ion Exch. Technol. 2012, 193-240. https://doi.org/10.5772/51040

[6] Ghosh P, Samanta AN, Ray S. Reduction of COD and removal of Zn2+ from rayon industry wastewater by combined electro-Fenton treatment and chemical precipitation. Desalination. 2011; 266(1-3):213-217. https://doi.org/10.1016/j.desal.2010.08.029

[7] Liu Q, Li Y, Chen H, et al. Superior adsorption capacity of functionalized straw adsorbent for dyes and heavy-metal ions. J. Hazard. Mater. 2020, 382. https://doi.org/10.1016/j.jhaz-mat.2019.121040

[8] Asere TG, Stevens CV, Du Laing G, Use of (modified) natural adsorbents for arsenic remediation: a review. Sci. Total Environ. 2019; 676:706–720. https://doi.org/10.1016/j.scitotenv.2019.04.237

[9] Xu H, Zhu S, Xia M, et al. Rapid and efficient removal of diclofenac sodium from aqueous solution via ternary core-shell CS@ PANI@ LDH composite: experimental and adsorption mechanism study. J. Hazard. Mater. 2021; 402. https://doi.org/10.1016/j.jhazmat.2020.123815 123815

[10] Xu H, Zhu S, Xia M, et al. Three-dimension hierarchical composite via in-situ growth of Zn/Al layered double hydroxide plates onto polyaniline-wrapped carbon sphere for efficient naproxen removal. J. Hazard. Mater. 2022; 423(B). https://doi.org/10.1016/j.jhazmat.2021.127192

[11] Xu Y, Zhang Q, Jiang G, et al. Activated Carbon Loaded with Ti3+ Self-Doped TiO2 Composite Material Prepared by Microwave Method. J. Mater. Eng. Perform. 2022; 31:2810–2822. https://doi.org/10.1007/s11665-021-06421-9

[12] Khan Z H, Gao M, Qiu W, et al. Mechanisms for cadmium adsorption by magnetic biochar composites in an aqueous solution. Chemosphere. 2020; 246. https://doi.org/10.1016/j.chemosphere.2019.125701125701.

[13] Khan A, Naeem A, Mahmood T, et al. Mechanistic study on methyl orange and congo red adsorption onto polyvinyl pyrrolidone modified magnesium oxide. Int. J. Environ. Sci. Technol. 2022; 19(4):2515–2528. https://doi.org/10.1007/s13762-021-03308-z

[14] Barakat M A. New trends in removing heavy metals from industrial wastewater. Arabian Journal of Chemistry. 2011;4(4):361-377.

[15] Guillaume Hopsort, Quentin Cacciuttolo, David Pasquier. Electrodialysis as a key operating unit in chemical processes: From lab to pilot scale of latest breakthroughs. Chemical Engineering Journal. 2024; 494:153111.

[16] Gmar S, Chagnes A, Lutin F, Muhr L. Application of Electrodialysis for the Selective Lithium Extraction Towards Cobalt, Nickel and Manganese from Leach Solutions Containing High Divalent Cations/li Ratio, Recycling. 2022; 7(2). https://doi.org/10.3390/recycling7020014

[17] Zimmermann P, Tekinalp O, Deng L, Wilhelmsen Ø, Burheim O S. Electrodialysis for Removal of Impurities in Silver Electrowinning, Meet. Abstr. 2023; MA2023-01:1608. https://doi.org/10.1149/ma2023-01241608mtgabs

[18] Kumar Y, Khalangre A, Suhag R, Cassano A. Applications of Reverse Osmosis and Nanofiltration Membrane Process in the Wine and Beer Industry. Membranes. 2025; 15:140.https://doi.org/10.3390/membranes15050140

[19] Charcosset C. Ultrafiltration, Microfiltration, Nanofiltration and Reverse Osmosis in Integrated Membrane Processes. In Integrated Membrane Systems and Processes; Basile A, Charcosset C, Eds. Wiley: Hoboken, NJ, USA. 2016, 1–22. ISBN 978-1-118-73908-2.

[20] Pati S, La Notte D, Clodoveo M L, Cicco G, Esti M. Reverse Osmosis and Nanofiltration Membranes for the Improvement of Must Quality. Eur. Food Res. Technol. 2014; 239:595–602.

[21] Poonguzhali E, Fathima Aadilah Mohamed Ali, Ashish Kapoor, Prabhakar S. Performance of membrane assisted solvent extraction with homologous solvents for the removal and recovery of phenol, Desalination and Water Treatment. 2022; 251:64-78. https://doi.org/10.5004/dwt.2022.28117

[22] Poonguzhali E, Ashish Kapoor, Prabhakar S. Membrane assisted process intensification and optimization for removal and recovery of phenol from industrial effluents, Separation and Purification Technology. 2023; 319:124026. https://doi.org/10.1016/j.seppur.2023.124026

[23] Sanika Bhokarikar, Poojitha P, Vijay Vaishampayan, Adithya Sridhar, Gurumoorthi P, Ashish Kapoor. Chapter Thirteen - Parameters affecting the efficiency of extraction systems in the food industries, Editor(s): Seid Mahdi Jafari, Sahar Akhavan-Mahdavi, In Unit Operation and Processing Equipment in the Food Industry, Extraction Processes in the Food Industry, Woodhead Publishing. 2024, 397-434. https://doi.org/10.1016/B978-0-12-819516-1.00010-7

[24] Ming Li, Chuanying Liu, Anting Ding, Chengliang Xiao, A review on the extraction and recovery of critical metals using molten salt electrolysis, Journal of Environmental Chemical Engineering. 2023; 11(3):109746. https://doi.org/10.1016/j.jece.2023.109746

[25] Yin T, Chen L, Xue Y, Zheng Y, Wang X, Yan Y, Zhang M, Wang G, Gao F, Qiu M. Electrochemical behavior and underpotential deposition of Sm on reactive electrodes (Al, Ni, Cu and Zn) in a LiCl-KCl melt, Int J. Min. Met. Mater. 2020; 27(12):1657–1665.

[26] Sun X, Chen Y, Liang L, Xie G, Peng Y. Research on Hydrocyclone Separation of Palygorskite Clay. Minerals. 2023; 13:1264. https://doi.org/10.3390/min13101264

[27] Baoyu Cui, Caie Zhang, Dezhou Wei, Shuaishuai Lu, Yuqing Feng. Effects of feed size distribution on separation performance of hydrocyclones with different vortex finder diameters, Powder Technology. 2017; 322:114-123. https://doi.org/10.1016/j.powtec.2017.09.010

[28] Aurélien Davailles, Eric Climent, Florent Bourgeois, Fundamental understanding of swirling flow pattern in hydrocyclones, Separation and Purification Technology. 2012; 92:152-160. https://doi.org/10.1016/j.seppur.2011.12.011

[29] Ghodrat M, Kuang SB, Yu AB, Vince A, Barnett GD, Barnett PJ. Numerical analysis of hydrocyclones with different conical section designs, Minerals Engineering. 2014; 62:74-84. https://doi.org/10.1016/j.mineng.2013.12.003

[30] Eldin Wee Chuan Lim, Yi-Ren Chen, Chi-Hwa Wang, Rome-Ming Wu. Experimental and computational studies of multiphase hydrodynamics in a hydrocyclone separator system, Chemical Engineering Science. 2010; 65(24):6415-6424. https://doi.org/10.1016/j.ces.2010.09.029

[31] Yin T, Xue Y, Yan Y, Ma Z, Ma F, Zhang M, Wang G, Qiu M. Recovery and separation of rare earth elements by molten salt electrolysis, Int J. Min. Met. Mater. 2021; 28(6):899–914.

[32] Irannajad M, Kamran Haghighi H. Removal of heavy metals from polluted solutions by zeolitic adsorbents: a review. Environmental Processes. 2021; 8:7-35. https://doi.org/10.1007/s40710-020-00476-x

[33] Bandura L, et al. Synthesis of zeolite-carbon composites using high-carbon fly ash and their ad-sorption abilities towards petroleum substances. Fuel. 2021; 283:119173. https://doi.org/10.1016/j.fuel.2020.119173